Lowland river responses to intraplate tectonism and climate forcing quantified with luminescence and cosmogenic ^{10}Be

JD Jansen[1], GC Nanson[2], TJ Cohen[2], T Fujioka[3], D Fabel[4], JR Larsen[5], AT Codilean[2], DM Price[2], HH Bowman[2], J-H May[2], LA Gliganic[2]

[1] Department of Physical Geography and Quaternary Geology, Stockholm University, 106 91 Stockholm, Sweden.
[2] School of Earth and Environmental Sciences, University of Wollongong, Wollongong 2500, Australia.
[3] Institute for Environmental Research, Australian Nuclear Science and Technology Organisation, Lucas Heights 2234, Australia.
[4] School of Geographical and Earth Sciences, University of Glasgow, Glasgow G12 8QQ, UK.
[5] School of Geography, Planning, and Environmental Management, University of Queensland, St Lucia 4072, Australia.

Abstract

Intraplate tectonism has produced large-scale folding that steers regional drainage systems, such as the 1600 km-long Cooper Ck, en route to Australia's continental depocentre at Lake Eyre. We apply cosmogenic ^{10}Be exposure dating in bedrock, and luminescence dating in sediment, to quantify the erosional and depositional response of Cooper Ck where it incises the rising Innamincka Dome. The detachment of bedrock joint-blocks during extreme floods governs the minimum rate of incision (17.4 ± 6.5 mm/ky) estimated using a numerical model of episodic erosion calibrated with our ^{10}Be measurements. The last big-flood phase occurred no earlier than ~112–121 ka. Upstream of the Innamincka Dome long-term rates of alluvial deposition, partly reflecting synclinal-basin subsidence, are estimated from 47 luminescence dates in sediments accumulated since ~270 ka. Sequestration of sediment in subsiding basins such as these may account for the lack of Quaternary accumulation in Lake Eyre, and moreover suggests that notions of a single primary depocentre at base-level may poorly represent lowland, arid-zone rivers. Over the period ~75–55 ka Cooper Ck changed from a bedload-dominant, laterally-active meandering river to a muddy anabranching channel network up to 60 km wide. We propose that this shift in river pattern was a product of base-level rise linked with the slowly deforming syncline-anticline structure, coupled with a climate-forced reduction in discharge. The uniform valley slope along this subsiding alluvial and rising bedrock system represents an adjustment between the relative rates of deformation and the ability of greatly enhanced flows at times during the Quaternary to incise the rising anticline. Hence, tectonic and climate controls are balanced in the long term.

Keywords

intraplate tectonism, bedrock river incision, anabranching, cosmogenic nuclides, luminescence, deposition rate.

Highlights

- We quantify fluvial response to intraplate tectonism with ^{10}Be and OSL-TL dating.
- Rare, extreme floods govern incision rate at the rising bedrock anticline.
- Tectonic and climate factors caused a planform shift to anabranching ~75–55 ka.
- Subsiding basins sequester most sediment en route to the continental depocentre.

1. Introduction

River response to tectonic deformation determines local relief and the supply of sediment to basins. Surface uplift may steepen rivers, increasing their erosional capacity to incise bedrock and transport sediment, but the converse also occurs, for instance, where rising transverse structures cause deposition and possible river diversion (Schumm et al., 2000). In the case of low relief landscapes, the sensitivity to small changes in slope means that anomalous river patterns may be the first clue to tectonic activity (e.g. Nanson, 1980). Intraplate tectonism has notably perturbed sections of large lowland rivers such as the Amazon and Mississippi chiefly because such rivers flow across very low gradients (Adams, 1980; Holbrook and Schumm, 1999). Whether a river is diverted or maintains course by incising in pace with uplift is held to be a function of the surface uplift rate, sediment flux, and stream power relative to critical thresholds of erosion (Schumm et al., 2000), though the role of the latter has been questioned (Humphrey and Konrad, 2000). Stream power fluctuations in large, low-gradient rivers are primarily a function of flood magnitude, yet episodic bedrock erosion via extreme floods has barely been examined in large lowland rivers. Much of what is known of how such rivers respond to transverse uplift derives from simplified scenarios explored via physical and numerical modeling (e.g., Humphrey and Konrad, 2000; Molnar et al., 2006), with flume experiments, in particular, contributing major insights to the effects of transverse uplift, such as changes in sinuosity and planform style (Ouchi, 1985; Schumm et al., 1987). Although such observations have been corroborated qualitatively in natural rivers (e.g. Nanson, 1980; Holbrook and Schumm, 1999), there is rarely sufficient constraint on the magnitude of deformation and the associated river responses to fully evaluate a natural experiment over 10^5–10^6 y timescales.

A transverse structure rising across the path of an unconfined river is generally predicted to cause deposition upstream of the uplift axis at the same time as erosion downstream (Ouchi, 1985; Humphrey and Konrad, 2000). To test this idea, we examine both modes of fluvial response along a large, lowland river in east-central Australia, Cooper Ck, where it crosses the anticline known as Innamincka Dome (Fig. 1). The rate of alluvial deposition is quantified with luminescence dating, and bedrock incision with *in situ* cosmogenic ^{10}Be. Based on analyses of i) river profile and planform, ii) spatial patterns of short and long-term deposition rates, and iii) rates of bedrock channel incision, we show that climate-driven flooding episodes over the last glacial cycle play a key role in how rivers adjust to intraplate tectonism, whilst sediment load appears secondary.

2. Field setting: Tectonism and drainage evolution of east-central Australia

The subdued relief across east-central Australia implies a relatively quiescent tectonic regime accordant with reports of low denudation rates <10 mm/ky based on cosmogenic nuclide measurements of bedrock surfaces in central Australia (e.g., Bierman and Caffee, 2002; Belton et al., 2004; Heimsath et al., 2010; Fujioka and Chappell, 2011). Yet, the continent as a whole has experienced appreciable Neogene-Quaternary tectonism given its intraplate setting (Sandiford et al, 2009). Surface uplift has generated major local relief in the Flinders Ranges where reverse faulting drives Plio-Quaternary slip rates of 20–150 mm/ky (Sandiford, 2003). The gross regional drainage patterns of east-central Australia are rooted in this Neogene-Quaternary tectonism, involving an array of low-amplitude, open fold structures (Senior et al., 1978; Wasson, 1983; Wells and Callen, 1986; Alley, 1998). Intraplate tectonism in Australia is attributed to far-field stresses at the plate-boundary coupled with upper mantle dynamics (Sandiford et al., 2004). The regional *in situ* stress field in east-central Australia has a maximum horizontal compressive stress azimuth running NE to SW (Hillis et al., 2008), a pattern that probably dates from at least the mid to late Miocene (Sandiford et al., 2004), explaining the orientation of synclinal structures that steer Cooper Ck and associated drainages for ~700 km. In its middle and lower reaches, Cooper Ck dissects two anticlinal structures formed in Mesozoic Eromanga Basin rocks: Innamincka Dome and Gason-Cooryanna Domes, which together exert major influence on landscape evolution east of the intra-continental depocentre at Lake Eyre (Fig. 1A). The wavelength of folding is ~20–50 km, and Tertiary uplift is estimated at ~200 m (Wopfner et al., 1974; Moussavi-Harami and Alexander, 1998), with neotectonism inferred by the thinning of Pliocene-Quaternary sediments over buried structures west of Innamincka Dome (Wasson, 1983; Moussavi-Harami and Alexander, 1998). Rates of Quaternary deformation however are not known, though impacts on river systems have been inferred (Rust, 1981; Rust and Nanson, 1986; Nanson et al., 2008; Waclawik et al., 2008).

2.1 Cooper Creek and Innamincka Dome

Cooper Ck drains ~300,000 km^2 of dryland east-central Australia. From the western slopes of the Great Dividing Range the Cooper flows ~1600 km inland to Lake Eyre, a large terminal playa draining ~14% of the continent (Fig. 1A). Mean annual rainfall ranges from 400–500 mm in

115 the headwaters to <100 mm at Lake Eyre. Flow is highly seasonal with long dry spells of low or
116 zero flow interspersed by high-magnitude flooding linked to the Indo-Australian monsoon and the
117 southeast trade-winds, both of which are modulated by the El Niño-Southern Oscillation (Kotwick
118 1986; Nanson et al., 2008). Considered to be the largest flood for >100 years (Kotwicki, 1986),
119 the February 1974 peak discharge was 24,970 m^3/s at Currareva, and 6360 m^3/s ~400 km
120 downstream at Cullyamurra (Fig. 1A,B), signifying ~75% transmission losses during this single
121 event (Knighton and Nanson, 2002).
122 Channel slope rarely exceeds 200 mm/km and longitudinal transitions in river style define
123 three reach segments: 1) the Cooper-Wilson synclinal depression, a vast anabranching channel
124 system 400 km long and up to 60 km wide; 2) Innamincka Dome, a mainly single-thread mixed
125 bedrock-alluvial channel with sporadic bedrock constrictions; and 3) Cooper Fan, which directs
126 drainage into several unconfined distributary channels with varying degrees of entrenchment
127 (Fig. 1B). Valley width contracts approaching the Innamincka Dome, and bedrock is first met at
128 Nappapethera waterhole where a single-thread Cooper Ck becomes confined between bedrock
129 banks with thin alluvial cover (Fig. 1B).
130 The local bedrock comprises Eyre Formation (Paleocene to Eocene) quartzose
131 sandstones underlain by Winton Formation (Cretaceous) kaolinitic shales and sandstones
132 (Wopfner et al., 1974)—all mildly folded with limbs dipping at 1–5°. A silicified palaeosol
133 developed prior to folding has formed a highly resistant silcrete duricrust sharply reflected in
134 valley constrictions culminating at the upstream end of Cullyamurra waterhole where flow
135 converges to ~30 m width (Fig. 1B). Such bedrock constrictions serve to amplify the erosional
136 capacity of large floods, and field observations confirm that large joint-blocks are episodically
137 plucked from bedrock outcrops (Fig. 2). Numerous large blocks (up to 1.1 m b-axis) are perched
138 on bedrock surfaces flanking Cullyamurra waterhole, many bearing unambiguous evidence of
139 flipping (e.g., inverted pot holes). The presence of such high-energy deposits in this very low
140 gradient and arid region motivates our efforts to determine the timing and magnitude of floods
141 necessary to erode bedrock and maintain course across the rising anticline.
142
143 **3. Methods**
144
145 *3.1 River profile and modern flood dynamics*
146
147 The longitudinal stream profile (Fig. 3A,B) was devised for Cooper Ck based on the Shuttle

Radar Topography Mission (SRTM, 1 arc-sec) digital elevation data (Supp. Data, S1). Valley cross-sections were measured at key bedrock constrictions in the field with a differential GPS (Trimble R7/R8), and Cullyamurra waterhole bathymetry was surveyed using a boat-mounted echo-sounder (Fig. 3C). The flow geometry detailed in 50 field-measured cross-sections was used to calibrate the HEC-RAS hydraulic model (HEC, 1997) through an 8 km reach, including the bedrock constriction at Cullyamurra waterhole (Supp. Data, S2). The 1974 peak discharge at Cullyamurra (6360 m^3/s, ~32-times the median annual flood) was simulated with the aim of estimating the erosional capacity of present-day big floods. Komar's (1996) selective entrainment function, a modified form of the Shields function, was employed to estimate the critical shear stress (τ_c, N/m^2) necessary for boulder mobility (cf Jansen, 2006):

$$\tau_c = 0.045\ (\rho_s - \rho)\ g\ d_{50}^{0.6}\ d^{0.4} \quad (1)$$

where ρ_s is boulder density (2650 kg/m^3), ρ fluid density (1000 kg/m^3), g gravity (9.8 m/s^2), d clast size (mm), and d_{50} the median size of surrounding clasts (assumed to be 500 mm).

3.2 Deposition rates quantified via OSL-TL dating and sediment load data

An inventory was compiled of 132 sedimentary units dated with optically-stimulated luminescence (OSL) and thermoluminescence (TL) from 80 natural exposures and drill-holes (Rust and Nanson, 1986; Nanson et al., 1988; Fagan, 2001; Coleman, 2002; Bowman, 2003; Maroulis et al., 2007; Nanson et al., 2008; Cohen et al., 2010) over an 820 km reach of Cooper Ck from Longreach to Merty Merty (Fig. 1A; note that Longreach is 200 km upstream of the extent shown). The inventory of ages (see Supp. Data, S3) was subdivided according to facies type: bedload (n=94) or overbank floodplain deposits (n=38), and long-term deposition rates (with a reduced dataset, see Results) were calculated by dividing depth by basal age assuming a 'zero age' at the surface. The presence of residual TL has been examined, but when converted to an age this rarely equates to more than a few millennia (Nanson et al., 2008, table 2), which is too small to have a significant effect on deposition rates for the timescales addressed here. The close correlation between 20 duplicate OSL-TL pairs (Supp. Data, S5) demonstrates that even single-grain aliquot OSL analyses do not produce systematically younger ages than TL.

With the aim of calculating vertical accretion rates of the modern floodplain for comparison to the luminescence-derived rates, concentrations of suspended-load sediment from flow gauges

at Currareva and Nappa Merrie (Nappapethera) were converted to a sediment volume delivered overbank to the floodplain each year (Supp. Data S4).

3.3 Fluvial bedrock incision rates quantified with cosmogenic ^{10}Be

The concentration of *in situ*-produced cosmogenic nuclides at the Earth's surface is a function of exposure ages and erosion rates (Lal, 1991; Gosse and Phillips, 2001). Surface exposure dating is widely employed to infer the exposure history of landscapes and to quantify the rate of fluvial incision into bedrock (e.g., Burbank et al., 1996; Jansen et al., 2011), though no studies specifically account for episodic plucking at the channel boundary. Four bedrock samples (CH1, -2, -3, -4) were collected for measurement of ^{10}Be in a cross-section spanning fluvially eroded bedrock surfaces at Cullyamurra waterhole—the Choke transect (Fig. 3,4)(see Supp. Data, S5) for full analytical information). The sampled surfaces preserve evidence of fluvial abrasion along with some local spalling and granular disintegration, but we interpret the stepped morphology of the cross-section to be chiefly the result of plucking of large silcrete joint-blocks (Fig. 2). The thickness of detached blocks is a function of the spacing of primary horizontal joints in the bedrock, which was estimated by measuring 50 joints in the sample transect.

4. Results

4.1 River profile and modern flood dynamics

Upstream of the Dome the anabranching channel network maintains a remarkably constant reach-slope of 176 ± 3 mm/km (mean ± 95% confidence interval) over 135 km from Shire Rd to the Choke transect (Fig. 3B). From here the channel steepens along a bedrock-confined reach culminating in an ~18 m-high knickpoint concealed beneath the water-level of Cullyamurra waterhole (Fig. 3C). The knickpoint tip lies 340 m downstream of the Choke, and corresponds to a bedrock-constriction 60 m in width (Fig. 3C,4). About 17 km further downstream the channel resumes a fully alluvial condition at the Cooper Fan apex and the mainstem flows west with a reach-slope of 153 ± 36 mm/km (mean ± 95% confidence interval) similar to that above the Dome.

The HEC-RAS model simulations of the 6360 m^3/s discharge (>100-year flood in 1974)

show that the flow hydraulics are strongly influenced by the degree of lateral constriction at the knickpoint. Floodwaters were estimated to be ~15 m deep at the Choke (Fig. 3C,4), and the zone of water-surface steepening corresponds to the deposits of coarse boulders on flanking bedrock surfaces (Fig. 2). The average intermediate axis of the four largest detached joint-blocks is 900 mm, which according to Komar's (1996) function, Eq. (1), yields a critical shear stress of 461 N/m^2. In comparison, the mean shear stress (cross-section average) predicted by the HEC-RAS model for the 6360 m^3/s discharge at the boulder site was 52 N/m^2, or ~11% of the critical threshold (Supp. Data, S2). This is probably a crude estimate, given that turbulence around irregular bedrock boundaries can produce widely variable localised flow conditions (Komar, 1996), but the results strongly imply that the largest joint-blocks at the Choke are mobilised by floods with annual exceedance probability of much less than 1%.

4.2 Deposition rates quantified via OSL-TL dating and sediment load data

The 132 OSL-TL dated sedimentary units are mostly <270 ka and from depths of <12 m, although the oldest age, 740 ± 55 ka, was obtained from a depth of 27 m (Supp. Data, S3). A frequency analysis based on kernel density estimates of those ages distributed upstream of Innamincka Dome indicates a transition beginning ~75 ka from sandy bedload facies to muddy top-stratum (Fig. 5A); hence, this threshold was chosen as the minimum bounding-age for calculating long-term deposition rates from basal bedload units. Ages <75 ka are excluded because they are considered to be influenced by the transition in river pattern from meandering to anabranching ~75–55 ka. Overbank deposition rates were calculated likewise from dated floodplain units using a minimum bounding age of 20 ka; units <20 ka are excluded because they likely reflect the influence of preservation bias, rather than indicating long-term deposition rates (Lewin and Macklin, 2003). The scaling between deposition rate and its measurement interval is a well known aspect of sedimentary environments (Sadler, 1981; Schumer and Jerolmack, 2009). The age-limiting thresholds (>75 ka for bedload, and >20 ka for floodplain) considerably enhance data reliability by helping to suppress the deposition rate–age scaling (Figs 5B, 6).

From relatively low, long-term values at Longreach (445 km), deposition rates become more variable downstream along the Cooper-Wilson synclinal basin (Fig. 6A). There is no steady downstream gradation in slope associated with the river profile: both vary widely, as shown by the lack of scaling between deposition rate and channel slope in this reach (Fig. 6B).

Downstream of ~870 km (Fig. 6A) and especially in the Wilson depression, deposition rates derived from basal bedload units vary widely from ~12 to 106 mm/ky; floodplain deposition rates reveal similar variation from ~20 to 111 mm/ky, although one outlier is 160 ± 12 mm/ky (at ~962 km, not shown in Fig. 6A). Accepting the broad spread of rates as being representative of the natural variation yields an average long-term deposition rate upstream of the Innamincka Dome of 48 ± 21 mm/ky (mean ± 1σ, n=23). Likewise, the average overbank deposition rate of 64 ± 33 mm/ky (mean ± 1σ, n=8, excluding outlier) overlaps with the bedload deposition rate above within one standard error. The modern rate of floodplain deposition derived from sediment load data is estimated at 48 ± 18 mm/ky, which is very close to the long-term rates above (Fig. 6A). Downstream of the Dome deposition rates appear to fall off rapidly to <20 mm/ky, as the sediment load is dispersed into three main distributaries: Cooper Ck main stem, Northwest branch, and Strzelecki Ck.

4.3 Fluvial bedrock incision rates quantified with cosmogenic ^{10}Be

The measured ^{10}Be concentrations on the lower three bedrock surfaces (CH2, -3, -4) are statistically equivalent within 1σ analytical errors, while that at CH1 is several-fold greater (Fig. 4, Table S5-1). Uniform nuclide concentrations measured at CH2, -3, -4 (spanning ~5 m of vertical section) suggest that these surfaces were probably eroded in the same event (or several floods closely-spaced in time) that caused widespread bedrock erosion along the valley margin, rather than being incrementally incised from high to low elevation. The stepped morphology of the sampled transect strongly suggests that large joint-blocks have been episodically plucked, with the minimum depth of plucking probably set by the spacing of primary horizontal joints measured in this study at 67 ± 24 cm (mean ± 1σ).

A simple episodic plucking model was developed to explore scenarios consistent with the measured ^{10}Be concentrations by varying the number of joint-blocks detached, and the time interval since detachment (Fig. 7A,B; see Supp. Data, S5). In brief, the model assumes: i) the nuclide concentration at CH1 reflects a steady-state bedrock erosion rate of 1.5 mm/ky, and CH2, -3, and -4 are subject to this background erosion rate for their entire exposure history; a rate that is representative of the local silcrete lithology and regional denudation; ii) nuclide concentrations at CH2, -3, and -4 are the result of episodic plucking of one, two or three joint-blocks (one block is 67 cm thick); iii) the timing of block detachment (T_d) was preceded by a period (T_i) in which cosmogenic nuclides accumulated in the sampled surfaces at a depth

defined by the thickness of overlying blocks (either 67, 134, or 201 cm); and iv) cosmogenic nuclides accumulated in the sampled surfaces prior to $T_i + T_d$ are negligible compared to those accumulated during T_i and T_d.

The model computes the timing of block detachment (T_d) for a given pre-detachment plucking interval (T_i) up to 150 ka (Fig. 7B). Maximum T_d indicates the earliest possible plucking episode, 112–121 ka, when T_i is zero (hence inheritance is zero), and the entire nuclide inventory is accumulated during the post-detachment period, T_d. As T_i increases, the proportion of the nuclide concentration attributable to the pre-detachment period grows, and the timing of the last plucking episode becomes younger. This effect on T_d is most pronounced when assuming detachment of a single block; a 67 cm joint-block shields only 68% of the cosmic-ray flux from underlying surfaces, whereas two or three blocks impart greater shielding (90% and 97%, respectively), so the fraction of inherited nuclides in the newly exposed surface is minimal in the latter cases (Fig. 7A,B). The resultant bedrock incision rate is dependent upon the number of joint-blocks detached: modelling one, two, or three blocks yields minimum incision rates of 5.8, 11.6 and 17.4 mm/ky, respectively (Supp. Data, S5). Given that the cumulative thickness of three joint-blocks (~2 m) approximates the height of bedrock steps between the CH2, -3 and -4 surfaces (Fig. 4), the removal of three blocks together (or in closely-spaced events) poses the most plausible scenario to explain the ^{10}Be concentrations measured on those surfaces. Hence the best estimate of the timing of detachment is close to the mean *maximum* T_d of ~117 ka, implying a *minimum* long-term bedrock incision rate of 17.4 ± 6.5 mm/ky (Supp. Data, S5).

5. Discussion

5.1 Estimated rates of anticlinal uplift and basin subsidence

Cooper Ck shows no evidence of channel steepening where it first meets bedrock at Nappapethera waterhole and forms a bedrock trench 10 m deep and 250 m wide (Fig. 1, 3B): a constant rectilinear slope is maintained for 135 km from Shire Rd to the Cullyamurra knickpoint (Fig. 3B). The Cooper has maintained its course across the anticlinal uplift at Innamincka Dome by incising bedrock at a minimum estimated rate of 17.4 ± 6.5 mm/ky, which greatly exceeds the background bedrock denudation rates of ~0.2–5 mm/ky typical of intraplate central Australia (e.g., Bierman and Caffee, 2002; Belton et al., 2004; Heimsath et al., 2010; Fujioka and Chappell, 2011), and our own measurement of 1.5 mm/ky at CH1, which is essentially the rate of

313 bedrock hillslope lowering. Such rates are significantly slower than ^{10}Be-derived fluvial incision
314 rates (~60–120 mm/ky) from the tectonically-active Flinders Ranges to the south (Quigley et al.,
315 2007).
316 It is generally the case that steepening and narrowing occurs where an alluvial river meets
317 bedrock due to the increased erosional capacity necessary to erode bedrock (Schumm et al.,
318 2000). Any relative uplift of the Dome should theoretically cause deposition rates to increase as
319 channel slopes decline towards the rising anticline. The lack of sensitivity of deposition rate to
320 channel slope is unexpected (Fig. 6B), and suggests that something other than slope must be
321 governing sedimentation. One explanation for the decoupling of slope and deposition rate is that
322 surface subsidence is accommodating the thickening valley fill and allowing Cooper Ck to
323 maintain a constant channel slope (cf Ouchi 1985). Large seasonal swamps upstream of
324 Nappapethera correspond to the area of widely varying deposition rates (Fig. 1B, 6A),
325 suggesting that spatially non-uniform surface subsidence might be reflecting intra-basinal
326 differences in compaction of the >100 m deep sediment pile.
327 Surface subsidence coupled with anticlinal uplift separates the aggrading basin upstream
328 from the erosion occurring at the knickpoint and bedrock constrictions, and the magnitude of
329 uplift relative to erosion can be estimated via simple geometric arguments; a schematic overview
330 is presented in Figure 8. Given that the bedrock channel bed at the Choke lies at 39.9 m asl (Fig.
331 3C), substantial relative vertical displacement can be deduced from the elevation of the base of
332 the >100 m thick basin-fill (Senior et al., 1978), which lies well below sea level. The absence of
333 channel steepening across the alluvial-bedrock transition suggests firstly that flow constriction
334 provides sufficient boost in erosional capacity to incise bedrock without steepening, and
335 secondly that long-term rates of fluvial incision and uplift must be approximately balanced. The
336 relative contribution of subsidence versus uplift is difficult to constrain with precision, but may be
337 estimated using end-member assumptions as follows. The subsidence-dominant case builds on
338 the condition that the average deposition rate upstream of the Dome (48 ± 21 mm/ky) wholly
339 reflects the accommodation space provided by basin subsidence, hence the fluvial incision rate
340 (17.4 ± 6.5 mm/ky) need only match the equivalent minimum rate of anticlinal uplift: ~17 mm/ky.
341 In the case of maximal anticlinal uplift and zero subsidence (with constant valley slope through
342 time), the average basin deposition rate (48 ± 21 mm/ky) plus the rate of fluvial incision (17.4 ±
343 6.5 mm/ky) gives an uplift rate of ~65 ± 22 mm/ky. In other words, back-tilting and the growth of
344 accommodation space associated with anticlinal uplift is the governing control on basin
345 deposition and bedrock erosion.

The Cooper Ck example of anticlinal uplift accompanied by synclinal subsidence poses significant additional complexity to the fault-bound block-uplift model proposed by Humphrey and Konrad (2000). Moreover, our results challenge Humphrey and Konrad's emphasis on the importance of sediment load over stream power concerning the erosional and depositional responses to transverse uplift. Firstly, sediment-driven abrasion is not significant for incision at the Dome; bedrock incision occurs via plucking, as dictated by thresholds of joint-block detachment that are well described by stream power or shear stress (Supp. Data, S2). Second, extremely slow regional denudation (~0.2–5 mm/ky) coupled with aridity produces very low sediment loads, yet the Cooper is still able to fill the accommodation space—maintain a linear stream profile—upstream of the Dome. This suggests that, contrary to Humphrey and Konrad (2000), sediment load is not a rate-limiting control on bed slope in the 'critical region' upstream of the uplift.

Rivers traversing east-central Australia are susceptible even to low rates of surface deformation due to extremely low channel slopes commonly <200 mm/km. The close accordance between folding and regional drainage points directly to the influence of structural control, and only the largest rivers, such as Cooper Ck and Diamantina River, have antecedent reaches that cut transverse to structure (Fig. 1A). Cullyamurra waterhole occupies a bedrock-confined trench that appears to be the product of the headward-retreating knickpoint that now stands at the waterhole's upstream limit (Fig. 3C). We speculate that the knickpoint was initiated at the faulted western margin of the anticline ~30 km to the west (Moussavi-Harami and Alexander, 1998). Notable seismicity has occurred in the vicinity of the Dome: 11 earthquakes of magnitude ≥3 and two ≥4, since the early-1960s (Fig. 1B). Other inferred evidence of recent deformation is the unchannelised reach of Strzelecki Ck at the fan apex (Fig. 1B). The knickpoint is a very pronounced 18 m-high step that dwarfs all other local convexities in the Cooper profile. Ongoing headward retreat to Nappapethera is predicted to instigate a major phase of erosion as the basin-fill upstream adjusts to lower base-level. Previous episodes of base level lowering may explain the fragments of planated bedrock observed at ~10 m above the modern channel observed upstream between Nappapethera and the Choke.

5.2. Tectonic and climatic influences on river pattern and sedimentation

Rising base-level is central to most models concerned with the origin and cause of anabranching, especially some well-studied North American examples (Smith and Smith, 1980;

379 Smith, 1983; Makaske et al., 2002), and this notion is further backed by flume experiments (e.g.,
380 Ouchi, 1985). Anabranching is not limited to areas experiencing rising base-level (Nanson and
381 Knighton, 1996), though such areas do host some extensive and well developed examples
382 (Nanson et al., 1986). Recent work on the problem focuses upon sediment transport capacity
383 and flow efficiency, with the proposal that division of flow and sediment into multiple channels
384 may be a mechanism for maximising sediment conveyance in low-gradient settings (Jansen and
385 Nanson, 2004, 2010; Huang and Nanson, 2007), or in the case of nonequilibrium systems, for
386 rapidly distributing sediment storage (Tabata and Hickin 2003; Jansen and Nanson, 2004).
387 Whereas the modern Cooper is a low-energy and predominantly suspended-load anabranching
388 system, the underlying Pleistocene sandy bedload signals a laterally-active meandering river
389 with a bankfull discharge ~5–7 times that of today (Nanson et al., 1986, 1988; Rust and Nanson,
390 1986). In line with flow efficiency arguments, the transition to anabranching between ~75–55 ka
391 (Fig. 5A) coincided with two factors that both diminish sediment transport capacity: decreasing
392 discharge due to climate, and declining valley slope due to surface deformation. Previous work
393 has attributed the high-energy meandering system to wetter conditions in Marine Isotope Stage-
394 5 (MIS-5: ~74–130 ka) and earlier, followed by gradual drying over the last glacial cycle, with
395 tectonism relegated to a secondary role (Rust, 1981; Rust and Nanson, 1986; Nanson et al.,
396 2008). However, in either case the transition to anabranching can be read as a counteract to the
397 fall in sediment transport capacity of the system (Jansen and Nanson, 2004). The anabranching
398 Cooper Ck maintains sediment conveyance across extremely low slopes of ~230–180 mm/km
399 (Fig. 3A), despite >75% transmission losses between Currareva and Cullyamurra waterhole
400 (Knighton and Nanson, 1994). Given the present-day situation in which even the 100-year flood
401 magnitude is insufficient to achieve significant boulder transport, we surmise that MIS-5 was a
402 time of enhanced discharge on the Cooper with high erosional capacity at the Dome.
403
404 *5.3 Climate-driven bedrock incision controls long-term sediment storage*
405
406 How one of the largest river systems in central Australia has maintained course over active
407 structures reveals much about the long-term inputs of sediment and discharge to Lake Eyre, the
408 intra-continental depocentre. The notable absence of a deep sedimentary record at Lake Eyre is
409 difficult to reconcile with its positioning at the depocentre since the early Miocene (Wells and
410 Callen, 1986). Previous work has invoked deflation during arid playa phases (Magee et al.,
411 2004), but the volume of material contained within the fringing dune fields falls well short of a

412 Neogene depocentre draining ~1.2 million km^2. We propose an alternative explanation in which
413 sediment is sequestered en route to the depocentre: back-tilting has created accommodation
414 space for sedimentation in synclinal basins, while in turn enhancing the rate of vertical accretion
415 by reducing sediment transport capacity (Ouchi, 1985; Holbrook and Schumm, 2000). With 100–
416 150 m of fluvial sands and muds (Senior et al., 1978), the Cooper-Wilson syncline contains
417 ~660–990 km^3 of sediment storage (assuming a prismatic basin geometry) between Currareva
418 and Nappapethera; a volume that dwarfs the 16–40 km^3 of post-Miocene sediments (assuming
419 2–5 m thickness over 8000 km^2) stored in Lake Eyre today. The syncline therefore acts as an
420 efficient sediment trap, explaining the low sediment delivery to Lake Eyre itself. The Cooper Ck
421 example demonstrates that even where tectonism is relatively modest, synclinal subsidence in
422 the path of lowland arid-zone rivers can foster multiple depocentres that overshadow sediment
423 volumes stored at topographic base level.
424 The low stream-power that is typical of large, low gradient rivers means that such rivers
425 can in some cases be dependent upon extreme floods to maintain sediment transport capacity
426 (cf Molnar et al., 2006). The subsiding Cooper-Wilson syncline provides considerable
427 accommodation space for sediments whose partial reworking is governed by the capacity of
428 large floods to lower base-level by incising bedrock obstructions downstream, and in this context
429 geomorphically-effective floods have an annual exceedance probability of much less than 1%.
430 ^{10}Be exposure dating suggests that major bedrock erosion due to high-magnitude floods most
431 likely occurred during MIS-5; timing that corresponds closely with independent OSL-TL evidence
432 of strong fluvial activity indicated by the frequency of dated bedload units (Fig. 5A). The implied
433 absence of Holocene incision at the Choke suggests that fluvial activity in central Australia does
434 not conform to a simple cycle of dry glacial and wet interglacial; rather, continental aridity may be
435 strengthening in the long-term (Nanson et al., 2008). It may be that aridity is underpinning a
436 decrease in the incision rate by suppressing the frequency of large floods (Molnar et al., 2006).
437
438 **6. Conclusions**
439
440 Large-scale folding associated with intraplate tectonism is responsible for deformation patterns
441 that steer the regional drainage as well as providing accommodation space for sequestering
442 large volumes of sediment en route to the intra-continental depocentre, Lake Eyre. One such
443 storage, the Cooper-Wilson syncline, contains ~660–990 km^3 of Quaternary sediment
444 accumulated at a rate of 48 ± 21 mm/ky since ~270 ka, while at the same time Cooper Ck has

maintained its course across the rising anticlinal limb of Innamincka Dome by incising bedrock at a minimum rate of 17.4 ± 6.5 mm/ky. The rate of Dome surface uplift is bracketed between 17–65 mm/ky, but very likely falls closer to the lower end of this range (accounting for a greater proportion of subsidence relative to uplift). The rising bedrock Dome constitutes the local base-level, and thereby governs the valley slope across the subsiding basin; yet, this base-level is ultimately controlled by the rate of bedrock lowering via detachment of joint-blocks during rare, extreme floods. The last big-flood phase occurred no earlier than ~112–121 ka, corresponding to a period of enhanced fluvial activity in central Australia (Nanson et al., 2008). Relative base-level rise coupled with climate-forced reduction in discharge over the last glacial cycle is responsible for the transition in river pattern ~75–55 ka from a bedload-dominant, laterally-active meandering river to the vast, muddy anabranching channel network of today. The entrapment of sediment in such subsiding basins may explain the lack of Quaternary sediment accumulated in the Lake Eyre depocentre, and moreover suggests that notions of a single primary depocentre at base-level may not apply to lowland, arid-zone rivers.

Acknowledgements

This research was funded by a UK Natural Environment and Research Council fellowship (NE/EO14143/1) to Jansen, and Australian Research Council Discovery Grants (DP1096911, DP130104023) to Nanson and colleagues. We thank Sheng Xu for conducting the AMS measurements at the Scottish Universities Environmental Research Centre, RJ Wasson for comments on an early draft, and EW Portenga for an insightful review.

References

Adams, J., 1980. Active tilting of the United States midcontinent: geodetic and geomorphic evidence. Geology, 8, 442–6.

Alley, N.F., 1998. Cainozoic stratigraphy, palaeoenvironments and geological evolution of the Lake Eyre Basin. Palaeogeography, Palaeoclimatology, Palaeoecology 144, 239–263.

Belton, D.X., Brown, R.W., Kohn, B.P., Fink, D., Farley, K.A., 2004. Quantitative resolution of the debate over antiquity of the central Australian landscape: implications for the tectonics and geomorphic stability of cratonic interiors. Earth and Planetary Science Letters, 219, 21–34.

Bierman, P.R., Caffee, M., 2002. Cosmogenic exposure and erosion history of Australian bedrock landforms. Geological Society of America Bulletin, 114, 787–803.

Bowman, H.H., 2003. The flow hydraulics of Cooper Creek through the Innamincka Dome. Unpublished BSc (Hons) thesis, School of Geosciences, University of Wollongong.

Burbank, D.W., Leland, J., Fielding, E., Anderson, R.S., Brozovic, N., Reid, M.R., Duncan, C., 1996. Bedrock incision, rock uplift, and threshold hillslopes in the northwestern Himalayas. Nature, 379, 505 –510.

Cohen, T.J., Nanson G.C., Larsen, J.R., Jones, B.G., Price D.M., Coleman, M., Pietsch, T.J., 2010. Late Quternary aeolian and fluvial interactions on the Cooper Creek fan and the association between linear and source-bordering dunes, Strzelecki Desert, Australia. Quaternary Science Reviews, 29, 455–471.

Coleman, M., 2002. Alluvial, aeolian and lacustrine evidence for climatic and flow regime changes over the past 250 ka, Cooper Creek near Innamincka, South Australia. Unpublished PhD thesis, School of Geosciences, University of Wollongong.

Fagan, S.D, 2001. Channel and floodplain characteristics of Cooper Creek, central Australia. Unpublished PhD thesis, School of Geosciences, University of Wollongong.

Fujioka, T., Chappell, J., 2011. Desert landscape processes on a timescale of millions of years, probed by cosmogenic nuclides. Aeolian Research, 3, 157–164.

Galloway, M.C., Senior, D., Cooper, R.D., 1971. Tickalara, Queensland, Sheet SH54-3, 1:250 000 Geological Series. Bureau of Mineral Resources, Geology and Geophysics.

Gosse, J.C., Phillips, F.M., 2001. Terrestrial in situ cosmogenic nuclides: theory and application. Quaternary Science Reviews, 20, 1475–1560.

Gravestock, D.I., Callen R.A., Alexander, E.M., Hill, A.J., 1995. Strzelecki, South Australia, Sheet SH54-2, 1:250 000 Geological Series. Department of Mines and Energy, South Australia, pp 49.

HEC, 1997. HEC-RAS River Analysis System v.2.0 Hydrologic Engineering Centre, United States Army Corps of Engineers, Davis, California.

Heimsath, A.M., Chappell, J. Fifield, K., 2010. Eroding Australia: rates and processes from Bega Valley to Arnhem Land. In: Bishop, P., Pillans, B. (Eds), Australian Landscapes, Geological Society, London Special Publications, 346, 225–241.

Hillis, R.R., Sandiford, M., Reynolds, S.D., Quigley, M.C., 2008. Present-day stresses, seismicity and Neogene-to-Recent tectonics of Australia's 'passive' margins: intraplate deformation controlled by plate boundary forces. In: Johnson, H., Dore, A.G., Gatliff, R.W., Holdsworth, R., Lundin, E.R., Ritchie, J.D. (Eds), The Nature and Origin of Compression in Passive Margins. Geological Society, London, Special Publications, 306, 71–90.

Holbrook, J., Schumm, S.A., 1999. Geomorphic and sedimentary response of rivers to tectonic deformation: a brief review and critique of a tool for recognising subtle epeirogenic deformation in modern and ancient settings. Tectonophysics, 305, 287–306.

Huang, H.Q., Nanson, G.C., 2007. Why some alluvial rivers develop an anabranching pattern, Water Resources Research, 43, W07441.

Humphrey, N.F., Konrad, S.K., 2000. River incision or diversion in response to bedrock uplift. Geology, 28, 43–46.

Jansen, J.D., Fabel, D., Bishop, P., Xu, S., Schnabel, C., Codilean, A.T., 2011. Does decreasing paraglacial sediment supply slow knickpoint retreat? Geology, 39, 543–546.

Jansen, J.D., Nanson, G.C., 2004. Anabranching and maximum flow efficiency in Magela Creek, northern Australia. Water Resources Research, 40, W04503.

Jansen, J.D., Nanson, G.C., 2010. Functional relationships between vegetation, channel morphology, and flow efficiency in an alluvial (anabranching) river. Journal of Geophysical Reseach, 115, F04030.

Knighton, A.D., Nanson, G.C., 1994. Flow transmission along an arid zone anastomosing river, Cooper Creek, Australia. Hydrological Processes 8, 137–154.

Knighton, A.D., Nanson, G.C., 2002. Inbank and overbank velocity conditions in an arid zone anastomosing river. Hydrological Processes, 16, 1771–1791.

Komar, P.D., 1996. Entrainment of sediments from deposits of mixed grain sizes and densities. In: Carling, P.A., Dawson, M.R., (Eds), Advances in Fluvial Dynamics and Stratigraphy. John Wiley and Sons, Chichester, pp. 127–181.

Kotwicki, V., 1986. Floods of Lake Eyre. Engineering and Water Supply Department, Adelaide. 99 pp.
Lal, D., 1991. Cosmic ray labeling of erosion surfaces: in situ nuclide production rates and erosion models. Earth and Planetary Science Letters, 104, 424–439.
Lewin, J., Macklin, M.G., 2003. Preservation potential for Late Quaternary river alluvium. Journal of Quaternary Science, 18, 107–120.
Magee, J.W., Miller, G.H., Spooner, N.A., Questiaux, D., 2004. Continuous 150 k.y. monsoon record from Lake Eyre, Australia: Insolation-forcing implications and unexpected Holocene failure. Geology, 32, 885–888.
Makaske, B., Smith, D.G., Berendsen, H.J.A., 2002. Avulsions, channel evolution, and floodplain sedimentation rates of the anastomosing upper Columbia River, British Columbia, Canada, Sedimentology, 49, 1049–1071.
Maroulis, J.C., Nanson, G.C, Price, D.M., Pietsch, T.J., 2007. Aeolian-fluvial interaction and climate change: source-bordering dune development over the past ~100 ka on Cooper Creek, central Australia. Quaternary Science Reviews, 26, 386–404.
Molnar P., Anderson, R.S., Kier, G., Rose, J., 2006. Relationships among probability distributions of stream discharges in floods, climate, bed load transport, and river incision. Journal of Geophysical Research, 111, F02001.
Moussavi-Harami, R., Alexander, E., 1998. Tertiary stratigraphy and tectonics, Eromanga Basin region. MESA Journal, 8, 32–36.
Nanson, G.C., 1980. A regional trend to meander migration. Journal of Geology, 88, 107–117.
Nanson G.C., Knighton, A.D., 1996. Anabranching rivers; their cause, character and classification, Earth Surface Processes and Landforms, 21, 217–239.
Nanson, G.C., Rust, B.R., Taylor, G., 1986. Coexistent mud braids and anastomosing channels in an arid-zone river: Cooper Creek, central Australia. Geology, 14, 175–178.
Nanson, G.C., Young, R.W., Price, D.M., Rust, B.R., 1988. Stratigraphy, sedimentology and late-Quaternary chronology of the Channel Country of western Queensland. In: Warner, R.F., (Ed.), Fluvial Geomorphology of Australia. Academic Press, Sydney, pp. 151–175.
Nanson, G.C., Price, D.M., Jones, B.G., Maroulis, J.C., Coleman, M., Bowman, H., Cohen, T.J., Pietsch, T.J., Larsen, J.R., 2008. Alluvial evidence for major climate and flow regime changes during the middle and late Quaternary in eastern central Australia. Geomorphology, 101, 109–129.
Ouchi, S., 1985. Response of alluvial rivers to slow tectonic movement. Geological Society of America Bulletin, 96, 504–515.
Quigley, M., Sandiford, M., Fifield, L.K., Alimanovic, A., 2007. Landscape response to intraplate tectonism: quantitative constraints from ^{10}Be nuclide abundances. Earth and Planetary Science Letters, 261, 120–133.
Rust, B.R., 1981. Sedimentation in an arid-zone anastomosing fluvial system: Cooper's Creek central Australia. Journal of Sedimentary Petrology, 51, 745–755.
Rust, B.R., Nanson, G.C., 1986. Contemporary and palaeochannel patterns and the late Quaternary stratigraphy of Cooper Creek southwest Queensland, Australia. Earth Surface Processes and Landforms, 11, 581–590.
Sadler, P.M., 1981. Sediment accumulation rates and the completeness of stratigraphic sections. Journal of Geology, 89, 569–584.
Sandiford, M., 2003. Neotectonics of southeastern Australia: linking the Quaternary faulting record with seismicity and in situ stress. In: Hillis, R. R., Muller, D. (eds), Evolution and Dynamics of the Australian Plate. Geological Society of Australia Special Publication, 22, 101–113.
Sandiford, M., Wallace, M., Coblentz, D., 2004. Origin of the in situ stress field in southeastern

Australia. Basin Research, 16, 325–338.
Sandiford, M., Quigley, M., de Broekert, P., Jakica, S. 2009. Tectonic framework for the Cainozoic cratonic basins of Australia. Australian Journal of Earth Sciences, 56, 5–18.
Schumer, R., Jerolmack, D.J., 2009. Real and apparent changes in sediment deposition rates through time. Journal of Geophysical Research, 114, F00A06.
Schumm, S.A., Mosley, M.P., Weaver, W.E., 1987. Experimental fluvial geomorphology. John Wiley, New York, 413 pp.
Schumm, S.A., Dumont, J.F., Holbrook, J.M., 2000. Active tectonics and alluvial rivers. Cambridge University Press, 276 pp.
Senior, D., 1969 Durham Downs, Queensland, Sheet SG54-15, 1:250 000 Geological Series. Bureau of Mineral Resources, Geology and Geophysics.
Senior, D., 1970. Barrolka, Queensland, Sheet SG54-11, 1:250 000 Geological Series. Bureau of Mineral Resources, Geology and Geophysics.
Senior, B.R., Mond, A., Harrison, P.L. (1978). The geology of the Eromanga Basin. Bureau of Mineral Resources Bulletin 1967, 102 p.
Smith, D.G., Smith, N.D., 1980. Sedimentation in anastomosed river systems: Examples from alluvial valleys near Banff, Alberta, Journal of Sedimentary Petrology, 50, 157–164.
Smith, D.G, 1983. Anastomosed fluvial deposits: modern examples from western Canada. In: Collinson J.D., Lewin, J. (Eds), Modern and Ancient Fluvial Systems, Special Publication No. 6 International Association of Sedimentologists. Blackwell Scientific Publications, Oxford, 155–168.
Tabata, K.K., Hickin, E.J., 2003. Interchannel hydraulic geometry and hydraulic efficiency of the anastomosing Columbia River, southeastern British Columbia, Canada, Earth Surface Processes Landforms, 28, 837–852.
Townsend, I.J., Thornton, R.C.N., 1975. Innamincka, South Australia, Sheet SG54-14, 1:250 000 Geological Series. Geological Survey of South Australia.
Waclawik, V.G., Lang, S.C., Krapf, C.B.E., 2008. Fluvial response to tectonic activity in an intra-continental dryland setting: The Neales River, Lake Eyre, central Australia. Geomorphology 102, 179-188.
Wasson, R.J. 1983. The Cainozoic history of the Strzelecki and Simpson dunefields (Australia), and the origin of the desert dunes. Zeitshrift für Geomorphologie Supplementbände, 45, 85–115.
Wells, R.T., Callen, R.A., (Eds) 1986. The Lake Eyre Basin – Cainozoic sediments, fossil vertebrates and plants, landforms, silcretes and climatic implications. Australasian Sedimentologists Group Field Guide Series No. 4., Geological Society of Australia, Sydney.
Wopfner, H., Callen, R., Wayne, K.H., 1974. The Lower Tertiary Eyre Formation of the southwestern Great Artesian Basin. Journal of the Geological Society of Australia, 21, 17–51.

FIGURES

Fig. 1

A) Field area in east-central Australia (modified after Wells and Callen, 1986), with Innamincka Dome (ID), Cooper Fan (CF), Tirari Fan (TF), Currareva (C), plus Cooper floodplain (mid-grey), and major playas (black). **B)** 450 km-long reach of Cooper Ck centred on Innamincka Dome. Yellow filled-circles denote sites of measured deposition rates from Mt Howitt (H) to Merty Merty (M); dark-grey fills denote seasonal swamps. Stars denote earthquake epicentres $M_L > 3$ (Geoscience Australia earthquake database, 1961–2012). Grey outlines show extent of Cretaceous (Winton Fm) and Tertiary rocks (Eyre/Glendower Fm), red lines denote anticlines/synclines (triangles indicate dip-direction) and major faults (stem indicates down-throw) (Senior, 1969, 1970; Galloway et al., 1971; Townsend et al., 1975; Gravestock et al., 1995).

Fig. 2

A) Oblique aerial Google Earth image of Cooper Ck anabranching channels upstream of Innamincka Dome, near Meringhina waterhole (flow top to bottom). **B)** Stepped bedrock morphology at Choke transect (Cullyamurra waterhole); foreground boulder is ~1 m in diameter. **C)** Abraded and plucked bedrock surface at Choke. **D)** Imbricated boulder slab at Choke, with hat (arrowed).

Fig. 3

A) Cooper Ck long profile derived from SRTM 1 arc-sec data, showing mainstem (Longreach to Lake Eyre) and Strzelecki Ck distributary (grey line) at distance from headwater divide. Reach-slopes (s in mm/km) based on linear regression of elevations at 1 km intervals. **B)** Detail of stream profile upstream of Innamincka Dome (Shire Rd to Choke, 135 km): constant rectilinear reach slope of 176 ± 3 mm/km (mean ± 95% confidence interval) via linear regression fitted to elevations at 1 km intervals. **C)** Detail of channel bed profile through Cullyamurra waterhole, including pronounced ~18 m-high subaqueous knickpoint revealed via bathymetric survey. The water-surface profile at 6360 m^3/s (1974 flood) was determined with the HEC-RAS hydraulic model.

Fig. 4

Cosmogenic nuclide sample transect at the Choke left (south) valley-margin formed in well-jointed silcrete bedrock. Samples span 9 vertical metres from edge of high terrace surface (CH1) down to just above low-flow channel (CH4). The measured ^{10}Be concentrations (x10^3 atoms/g) are given with 1σ analytical errors (Supp. Data, S5). The simulated water-surface level for a discharge of 6360 m^3/s (1974 flood) is shown topping CH1. Full valley cross-section is inset.

Fig. 5

A) Luminescence-ages of bedload (n=49) and floodplain (n=37) sedimentary units (Supp. Data, S3) on Cooper Ck upstream of Innamincka Dome plotted as kernel density estimates (composite of Gaussian probability curves for each age normalized to unit area). The present-day anabranching channel network is entrenched within a floodplain mud sheet of ~2 to 6 m thickness, underlain by predominantly sandy bedload facies (Rust and Nanson, 1986)—all dates derive from this relatively uniform stratigraphy. During laterally-active channel phases the mud sheet was reworked across the full valley floor; however, from ~75 ka (denoted by dashed line) lateral migration began to decline, expanding the area of mud sheet preservation and leading eventually to the vertical-accretion floodplain and anabranching river pattern of today. **B)** Deposition rate versus age for bedload (black) and floodplain (grey) units, with 1σ errors. As shown here, imposing age-limiting thresholds (>75 ka for bedload, and >20 ka for floodplain units) considerably enhances data reliability by suppressing the scaling that normally exists between deposition rate and measurement interval (Supp. Data, S3).

Fig. 6

A) Downstream distribution of Cooper Ck deposition rates from Longreach (445 km) across Innamincka Dome to Merty Merty (1269 km on the Strzelecki Ck distributary). Open circles are deposition rates (mm/ky ± 1σ, n=38) derived from bedload sedimentary units >75 ka. Grey circles are overbank deposition rates (mm/ky ± 1σ, n=8) derived from floodplain sedimentary units >20 ka. Note that one floodplain outlier is not shown: 160 ± 12 mm/ky (at ~962 km). The modern floodplain deposition rate is 48 ± 18 mm/ky, as derived from sediment load data (Supp. Data, S4). **B)** Deposition rate versus channel slope (derived from a 5-km moving window) for bedload units (open circles, n=23) and floodplain units (grey circles, n=8) upstream of the Innamincka Dome.

Fig. 7

A) Schematic outline of the joint-block detachment model showing cosmogenic nuclides accumulating in two stages. For Stage 1, ^{10}Be accumulates relative to shielding depth, as determined by the number of overlying joint-blocks for period T_i — until high-intensity floods detach joint-blocks at time T_d. Nuclide accumulation beneath one, two, or three joint-blocks is denoted by blue dots, whose size indicates the degree of nuclide inheritance. For Stage 2, ^{10}Be accumulates at the exposed surface for period T_d indicated by red dot. The total concentration of ^{10}Be, at the time of sampling, is the sum of inheritance (blue dot) and post-detachment (red dot) components (see Supp. Data, S5). **B)** Results of the joint-block detachment model: time of detachment (T_d) versus pre-detachment interval (T_i) based on ^{10}Be concentrations at CH2, -2, and -3.

Fig. 8

Diagrammatic sketch of Cooper Ck across the Cooper-Wilson synclinal depression to Innamincka Dome (flow from left to right). Cooper Ck maintains a rectilinear channel slope across the subsiding basin by vertically aggrading. The knickpoint (KP) is in the process of retreating upstream towards the alluvial-bedrock transition at Nappapethera (Fig. 1B).

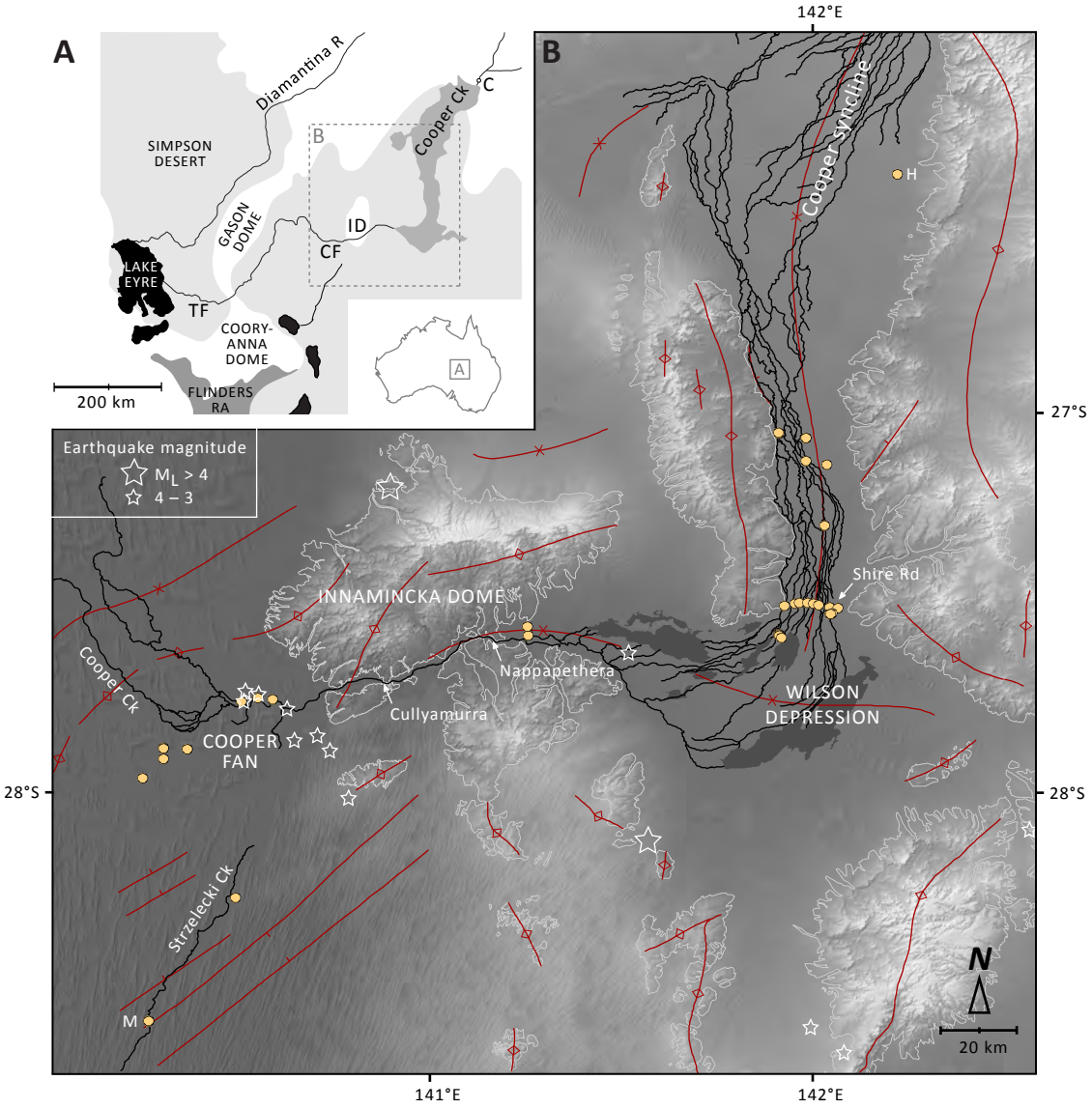
A
B
Diamantina R
Cooper Ck
SIMPSON DESERT
GASON DOME
ID
CF
LAKE EYRE
TF
COORY-ANNA DOME
FLINDERS RA
200 km
A
Earthquake magnitude
ML > 4
4 – 3
142°E
Cooper syncline
H
27°S
Shire Rd
INNAMINCKA DOME
Nappapethera
Cullyamurra
WILSON DEPRESSION
Cooper Ck
COOPER FAN
28°S
Strzelecki Ck
M
N
20 km
141°E
142°E

Fig. 1

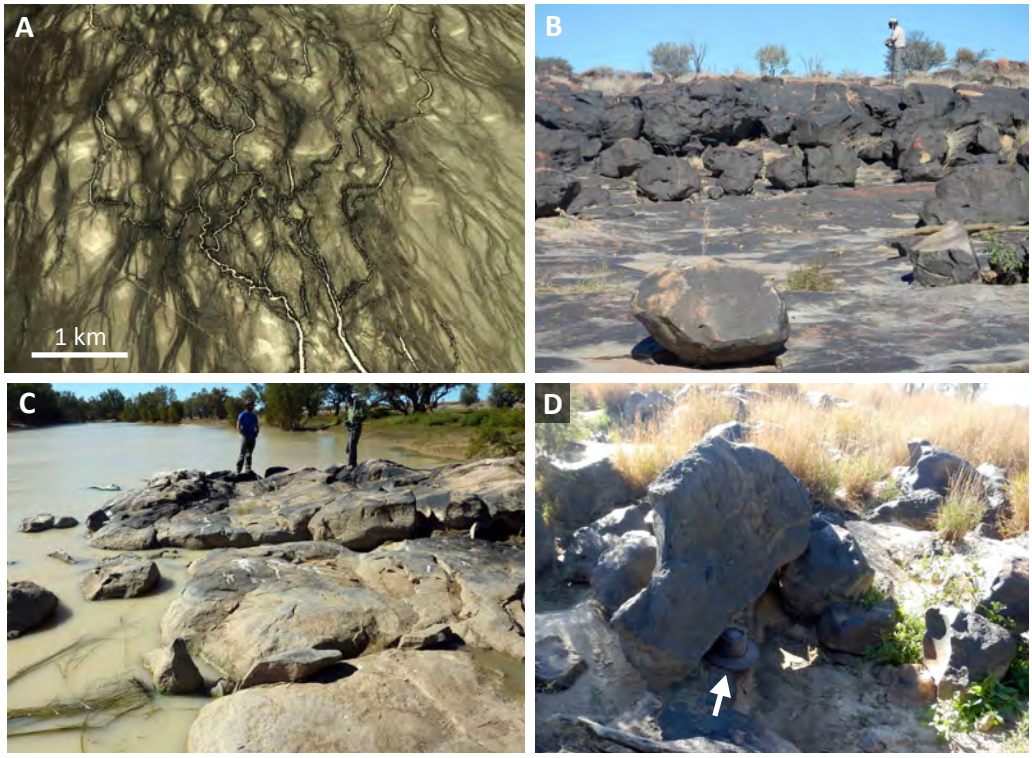

Fig. 2

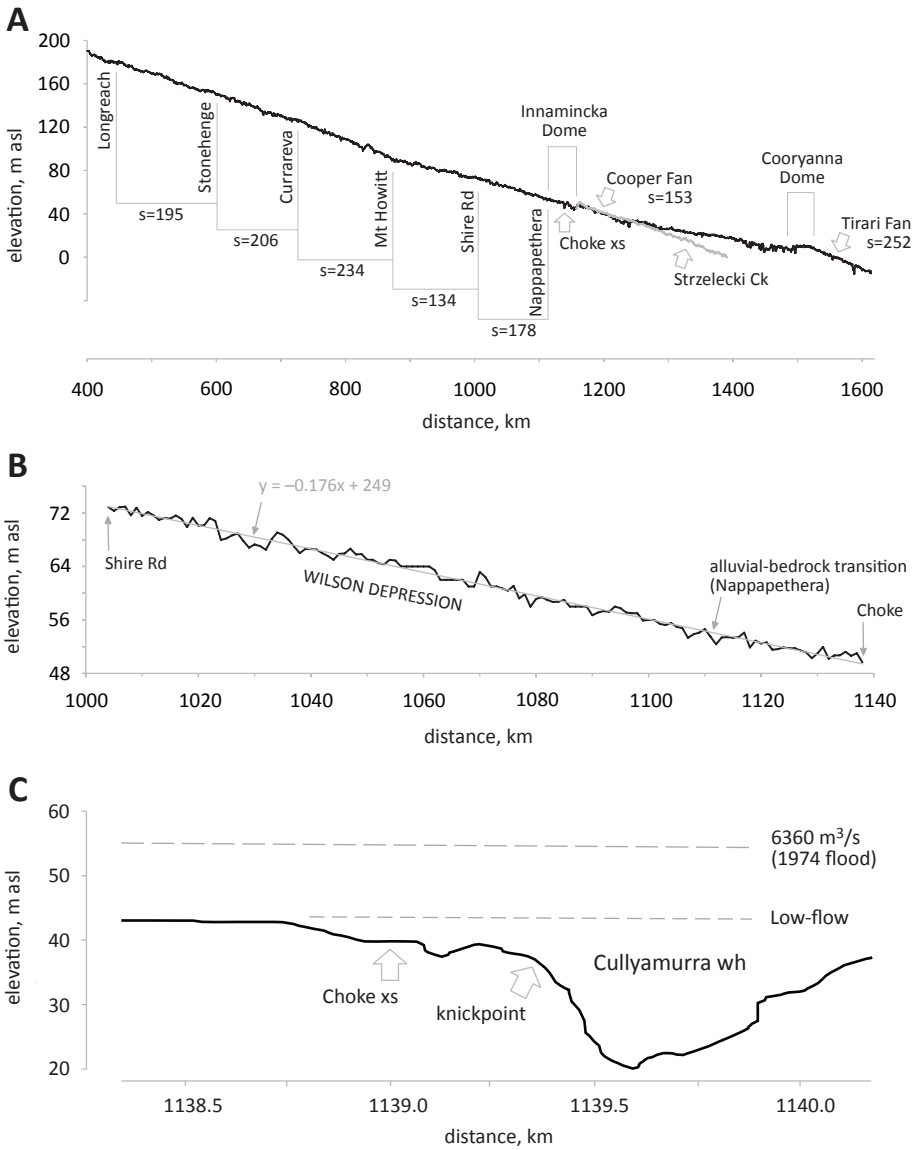
A
elevation, m asl
200
160
120
80
40
0
Longreach
Stonehenge
Currareva
Mt Howitt
Shire Rd
Nappapethera
s=195
s=206
s=234
s=134
s=178
Innamincka Dome
Cooper Fan s=153
Choke xs
Strzelecki Ck
Cooryanna Dome
Tirari Fan s=252
400
600
800
1000
1200
1400
1600
distance, km
B
elevation, m asl
y = –0.176x + 249
Shire Rd
WILSON DEPRESSION
alluvial-bedrock transition (Nappapethera)
Choke
72
64
56
48
1000
1020
1040
1060
1080
1100
1120
1140
distance, km
C
elevation, m asl
60
50
40
30
20
6360 m3/s (1974 flood)
Low-flow
Cullyamurra wh
Choke xs
knickpoint
1138.5
1139.0
1139.5
1140.0
distance, km

Fig. 3

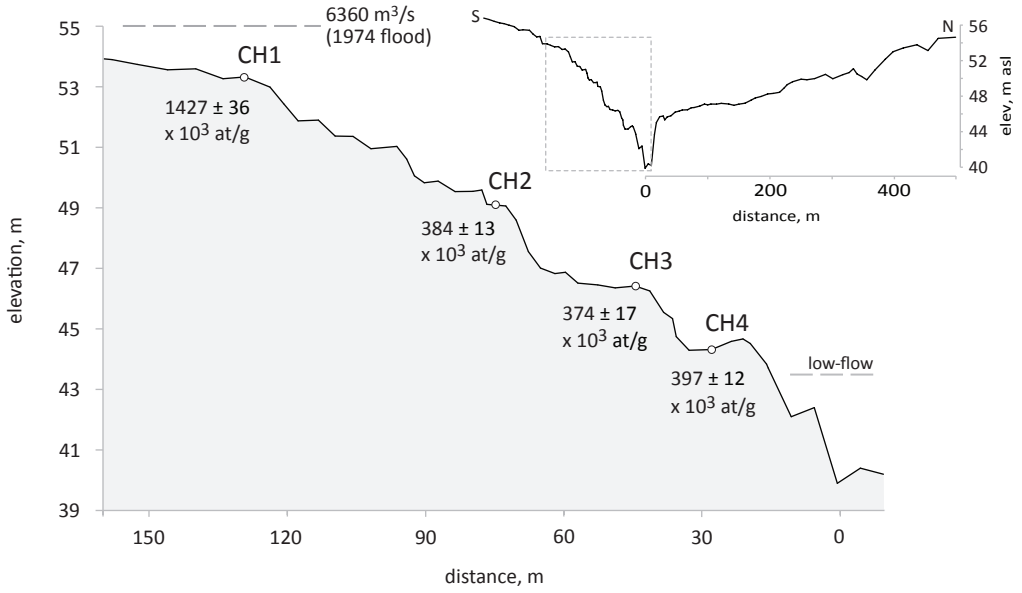
6360 m3/s
(1974 flood)
CH1
1427 ± 36
x 10^3 at/g
CH2
384 ± 13
x 10^3 at/g
CH3
374 ± 17
x 10^3 at/g
CH4
397 ± 12
x 10^3 at/g
low-flow
elevation, m
distance, m
S
N
elev, m asl
distance, m

Fig. 4

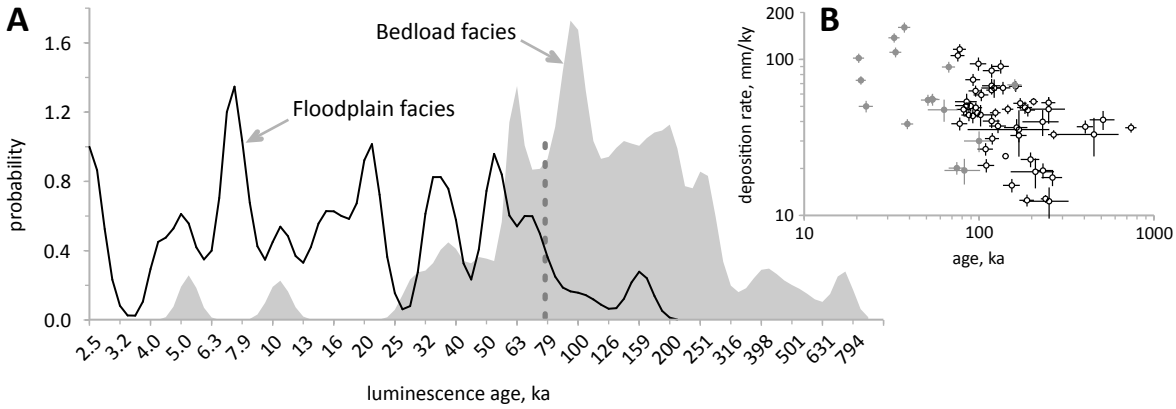
A
Bedload facies
Floodplain facies
probability
1.6
1.2
0.8
0.4
0.0
2.5
3.2
4.0
5.0
6.3
7.9
10
13
16
20
25
32
40
50
63
79
100
126
159
200
251
316
398
501
631
794
luminescence age, ka
B
deposition rate, mm/ky
200
100
10
10
100
1000
age, ka

Fig. 5

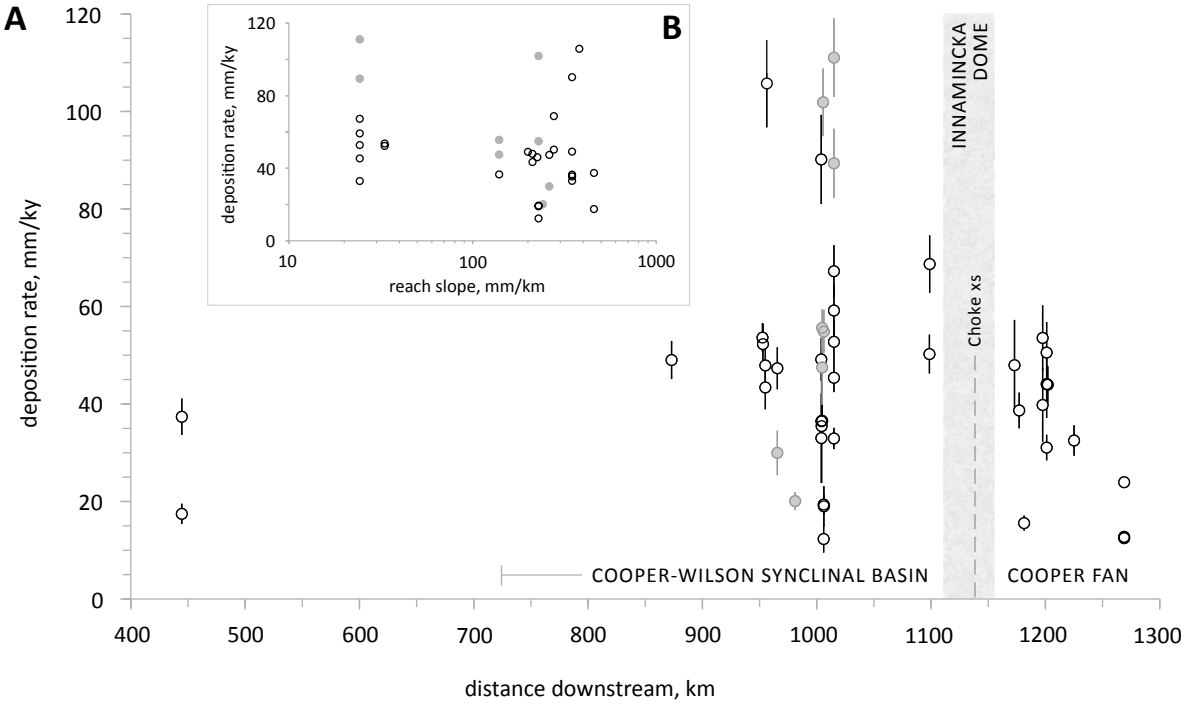
A
B
deposition rate, mm/ky
distance downstream, km
reach slope, mm/km
INNAMINCKA DOME
Choke xs
COOPER-WILSON SYNCLINAL BASIN
COOPER FAN

Fig. 6

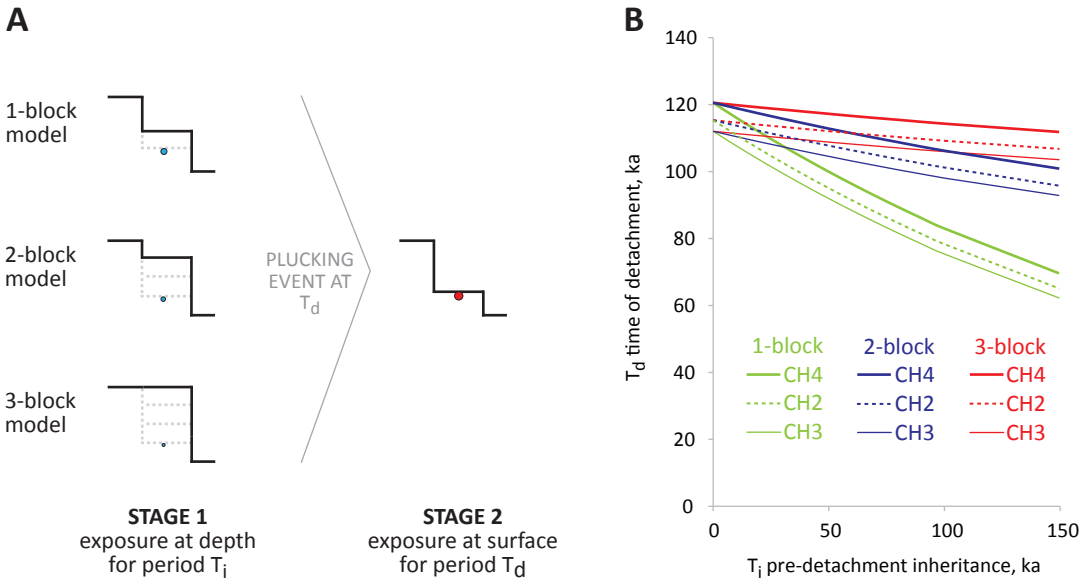
A
1-block model
2-block model
3-block model
PLUCKING EVENT AT T_d
STAGE 1
exposure at depth for period T_i
STAGE 2
exposure at surface for period T_d
B
T_d time of detachment, ka
T_i pre-detachment inheritance, ka
0
20
40
60
80
100
120
140
0
50
100
150
1-block
2-block
3-block
CH4
CH2
CH3

Fig. 7

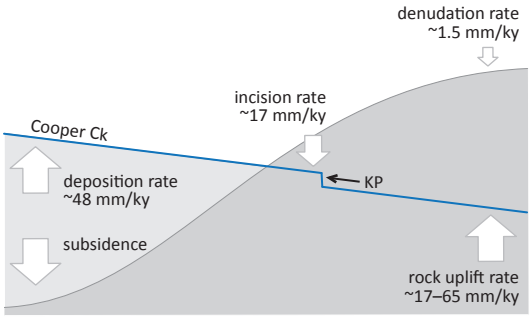
denudation rate
~1.5 mm/ky
incision rate
~17 mm/ky
Cooper Ck
deposition rate
~48 mm/ky
KP
subsidence
rock uplift rate
~17–65 mm/ky

Fig. 8